

## TITLE:

Non-parametric kernel density estimation of magnitude distribution for the analysis of seismic hazard posed by anthropogenic seismicity

## AUTHORS:

Francis Tong<sup>a</sup>, Stanisław Lasocki<sup>b</sup>, Beata Orlecka-Sikora<sup>c</sup>

<sup>a</sup> Institute of Geophysics, Polish Academy of Sciences, ORCID: 0000-0002-3849-884X

<sup>b</sup> Institute of Geophysics, Polish Academy of Sciences, ORCID: 0000-0002-3443-6473

<sup>c</sup> Institute of Geophysics, Polish Academy of Sciences, ORCID: 0000-0002-0182-1455

## Abstract

Frequent significant deviations of the observed magnitude distribution of anthropogenic seismicity from the Gutenberg-Richter relation require alternative estimation methods for probabilistic seismic hazard assessments. We evaluate five nonparametric kernel density estimation (KDE) methods on simulated samples drawn from four magnitude distribution models: the exponential, concave and convex bi-exponential, and exponential-Gaussian distributions. The latter three represent deviations from the Gutenberg-Richter relation due to the finite thickness of the seismogenic crust and the effect of characteristic earthquakes. The assumed deviations from exponentiality are never more than those met in practice.

The studied KDE methods include Silverman's and Scott's rules with Abramson's bandwidth adaptation, two diffusion-based methods (ISJ and diffKDE), and adaptiveKDE, which formulates the bandwidth estimation as an optimization problem. We assess their performance for magnitudes from 2 to 6 with sample sizes of 400 to 5000, using the mean integrated square error (MISE) over 100,000 simulations. Their suitability in hazard assessments is illustrated by the mean of the mean return period (MRP) for a sample size of 1000.

Among the tested methods, diffKDE provides the most accurate cumulative distribution function estimates for larger magnitudes. Even when the data is drawn from an exponential distribution, diffKDE performs comparably to maximum likelihood estimation when the sample size is at least 1000. Given that anthropogenic seismicity often deviates from the exponential model, we recommend using diffKDE for probabilistic seismic hazard assessments whenever a sufficient sample size is available.

## Introduction

The earthquake magnitude distribution is an essential component of probabilistic seismic hazard analysis. For this reason, the accurate modeling of this distribution is of paramount importance.

The most used magnitude distribution model is the exponential distribution. It results from the Gutenberg-Richter (G-R) magnitude-frequency relation  $\log n(M) = a - bM$ , where  $n(M)$  is the number of earthquakes having magnitudes from the bin centered at  $M$ , and  $a$  and  $b$  are constants (Gutenberg and Richter, 1954). The probability density function (PDF) of this model reads

$$f(M) = \begin{cases} 0 & \text{for } M < M_{min} \\ \beta e^{-\beta(M-M_{min})} & \text{for } M \geq M_{min} \end{cases} \quad (1)$$

where  $\beta = b \ln 10$ ,  $b$  is the G-R b-value, and  $M_{min}$  is the catalog completeness level, i.e., the magnitude value from which all earthquakes are in the catalog.

Recent studies of anthropogenic seismicity have shown that the observed magnitude distributions often deviate from exponential models. Furthermore, the observed distributions may exhibit complex, multimodal structures for which no parametric model can be proposed (Kostoglou et al., 2024, and the references therein). As things are, non-parametric kernel density estimation (KDE) (Silverman, 1986) has been proposed (e.g., Kijko, et al., 2001; Lasocki and Orlecka-Sikora, 2008) as it makes no assumptions about the form of the magnitude distribution.

Within the field of KDE, there are progressively more sophisticated implementations. We studied five newer ones to indicate the most suitable KDE for the specific case of magnitude distribution estimation. These were Scott's rule (Scott, 1992) and Silverman's rule (Silverman, 1986) with Abramson's adaptive bandwidth method (Abramson, 1982), the improved Sheather-Jones method (ISJ, Botev et al., 2010), the diffKDE method (Pelz et al., 2023), and the adaptiveKDE method (Shimazaki and Shinomoto, 2010).

We tested the KDE methods on synthetic data generated from three magnitude distribution models: exponential, bi-exponential, and exponential-Gaussian. The latter two distributions model magnitude distributions whose deviations from the Gutenberg-Richter relation result from physical hypotheses on the seismic processes.

Of the tested methods, the diffKDE turned out to be the best one overall. We also compared the KDE estimates to the MLE estimates obtained when assuming the data follows the Gutenberg-Richter relation; hence, its distribution is exponential. Our simulations showed that when the sample's underlying distribution is not exponential, KDE generally outperforms MLE, and the diffKDE method can be safely used even if the magnitude distribution is exponential.

## Materials and methods

### Kernel Density Estimation

Kernel density estimation (KDE) is a nonparametric statistical method for the estimation of probability density functions (PDFs). The kernel density estimator for a sample  $x = \{x_1, x_2, \dots, x_n\}$  is defined as (e.g., Silverman, 1986):

$$\hat{f}(x) = \frac{1}{nh} \sum_{i=1}^n K\left(\frac{x-x_i}{h}\right) \quad (2)$$

where:

$\hat{f}(x)$  is the KDE approximation of the true probability density  $f$ ,

$K(x)$  is the kernel function,

$h$  is the bandwidth.

The kernel function can be any symmetric, non-negative function that integrates to 1. There are many choices for the kernel function. Since the distribution models considered in this study had semi-infinite supports, we used exclusively the Gaussian kernel,

$$K(x) = \frac{1}{\sqrt{2\pi}} e^{-\frac{1}{2}x^2} \quad (3)$$

as it ensured the infinite support of  $\hat{f}(x)$ . For this kernel, the KDE estimates of the PDF and cumulative distribution function (CDF) are, respectively:

$$\hat{f}(x) = \frac{1}{nh\sqrt{2\pi}} \sum_{i=1}^n \exp\left[-\frac{(x-x_i)^2}{2h^2}\right] \quad (4)$$

$$\hat{F}(x) = \frac{1}{n} \sum_{i=1}^n \Phi\left(\frac{x-x_i}{h}\right) \quad (5)$$

where  $\Phi(\xi) = \frac{1}{\sqrt{2\pi}} \int_{-\infty}^{\xi} e^{-t^2/2} dt$  is the standard normal CDF.

The kernel density estimator is local. When the PDF of the random variable,  $X$ , is sharply zeroed outside a semi-finite interval  $[x_*, \infty)$ , which is the case of magnitude distribution (1), then the estimate (4) would have a spurious mode close to  $x_*$ , tending to zero at  $x_*$ . In such cases, the data sample  $x = \{x_1, x_2, \dots, x_n\}$  is mirrored symmetrically around  $x_*$  constructing the new sample  $x' = \{2x_* - x_n, \dots, 2x_* - x_2, 2x_* - x_1, x_1, x_2, \dots, x_n\}$  whose KDE estimate, (4), is  $\hat{f}'(x)$ . The PDF of  $X$  is  $\hat{f}(x) = 2\hat{f}'(x)$ .

The bandwidth,  $h$ , determines how much smoothing is applied to the density, and its choice affects the resultant estimate more than the choice of kernel function. There are many ways to select the bandwidth  $h$ . The five used in this paper are presented below.

#### Scott's rule

Under the assumption that the data follows a normal distribution, Scott derived an optimal bandwidth as:

$$h = \left(\frac{4}{3}\right)^{\frac{1}{5}} \sigma n^{-1/5} \quad (6)$$

where  $\sigma$  is the standard deviation of the data and  $n$  is the sample size (Scott, 1992).

#### Silverman's rule

For data that is close to normal, Silverman proposed the following rule of thumb:

$$h = 0.9 \min\left(\sigma, \frac{IQR}{1.34}\right) n^{-1/5} \quad (7)$$

where  $\sigma$  is the standard deviation of the data, IQR is the interquartile range, and  $n$  is the sample size (Silverman, 1986) .

#### Adaptive Bandwidths to correct Scott's and Silverman's rules

Magnitude distributions are exponential-like. Samples drawn from such distributions are unevenly populated, with sparse data from tails. The Gaussian kernel density estimator (4), with a constant bandwidth as in Scott's and Silverman's rules (6), (7), produces spurious irregularities in the intervals where data is sparse (Botev et al., 2010). On the other hand, accurate estimation of the tail of an earthquake magnitude distribution is crucial for accurate estimation of extreme event exceedance probabilities, which is, in fact, the target of seismic hazard assessment.

The problem due to the sparsity of data in some intervals, e.g., in tails like in the case of earthquake magnitudes, can be alleviated by methods that adapt kernel widths locally at the data points (e.g., Loftsgaarden and Quesenberry, 1965; Breiman et al., 1977; Abramson, 1982; Silverman, 1986; Izenman, 1991 and the references therein; Terrell and Scott, 1992).

We complete Scott's and Silverman's rules with Abramson's adaptive bandwidth method (Abramson, 1982). The bandwidth is adjusted by a factor inversely proportional to the square root of the density estimate. In effect, this reduces the bandwidth where there are many samples and increases it where samples are sparse.

In our case, it is implemented as follows:

- 1) Compute a pilot density estimate  $\tilde{f}(M_j)$  by convolution of the binned relative frequencies with a Gaussian filter
- 2) Calculate the geometric mean  $g$  of the pilot density estimates at each point,  $\{\tilde{f}(M_j)\}_{j=1}^n$

The bandwidth for the kernel centered at  $M_j$  is then:

$$h_j = h_0 \left( \frac{g}{\tilde{f}} \right)^{-\alpha} \quad (8)$$

where

$h_0$  is the bandwidth obtained from a fixed bandwidth selection method (Silverman or Scott)

$g$  is the geometric mean of the pilot density estimates

$\tilde{f}$  is the pilot density estimate

$\alpha$  is the sensitivity factor

Abramson indicated  $\alpha = 0.5$  as an optimal choice.

#### Improved Sheather-Jones (ISJ) and DiffKDE methods

Botev et al. (2010) proposed the Improved Sheather-Jones (ISJ) bandwidth estimation method, in which they exploited the fact that the Gaussian kernel is a fundamental solution to the heat diffusion partial differential equation (PDE) in  $x$  and time  $t$

$$\frac{\partial}{\partial t} u(x, t) = \frac{1}{2} \frac{\partial^2}{\partial x^2} u(x, t) \quad (9)$$

Their adaptive kernel density estimation is based on the smoothing properties of the linear diffusion process.

The approach of Botev et al. (2010) was further developed by Peltz et al. (2023). Their diffusion-based KDE (diffKDE) allows for adjusting the diffusion intensity (adaptive smoothing) in space.

#### AdaptiveKDE

Another way to create an adaptive bandwidth estimator is to reformulate it as an optimization problem. Shimazaki and Shinomoto (2010) proposed minimizing the L2 loss function between the kernel estimate and the true density function. Unlike Abramson's method, which varies the bandwidth only at sample points, this method returns variable bandwidth values across the domain where the data is provided. Performing successive iterations of optimization within each local interval will return an optimal bandwidth for each interval.

## Synthetic catalogs

We tested the performance of the five KDE methods on synthetic catalogs. The catalog data was drawn from exponential distributions and probabilistic models representing the observed and physically justified deviations of earthquake magnitude distributions from the G-R relation. Sampling was done using the inverse transform method, and  $10^5$  simulations were performed for each model distribution.

### Exponential Distribution

The PDF of the exponential distribution model of magnitude is (1). We studied the exponential model with the parameters  $b = 0.7, 1.0, 1.3$ , and  $M_{min} = 0.5$  (Figure 1).

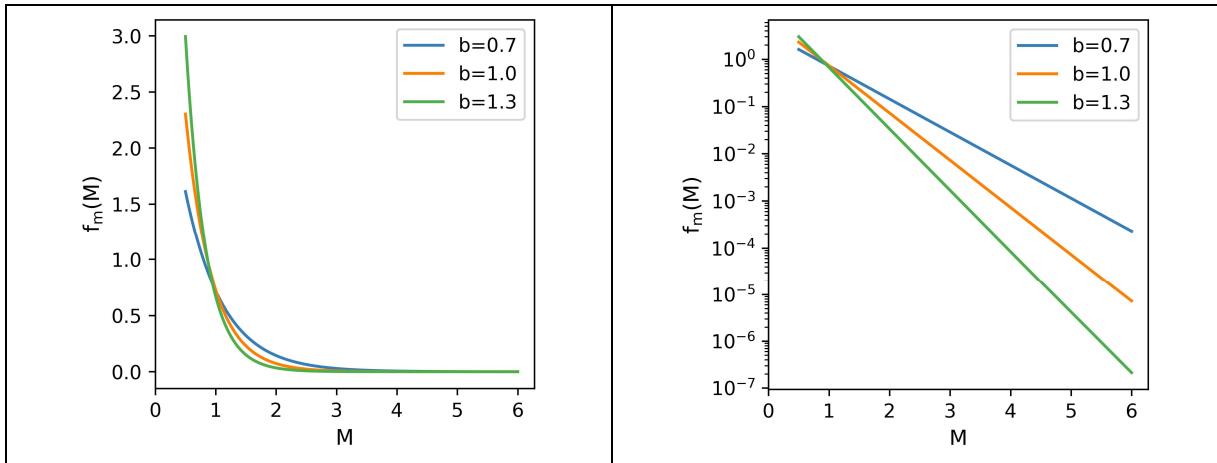


Figure 1 Exponential distribution models used to generate synthetic catalogs.

### Bi-exponential Distribution

The bi-exponential distribution results from the bi-linear frequency-magnitude relation

$$\log n(M) = \begin{cases} a_1 - b_1 M & \text{for } M \leq M_t \\ a_2 - b_2 M & \text{for } M > M_t \end{cases} \quad (10)$$

(Utsu, 1999). Its convex form,  $b_1 < b_2$ , models a change of the frequency distribution from small to large events resulting from the finite thickness of the seismogenic crust, which discriminates large events. (e.g., Pacheco et al., 1992; Okal and Romanowicz, 1994; Sornette and Sornette, 1999). However, in anthropogenic seismicity, there is observational evidence of both convex and concave bi-linearity (e.g., Kijko et al., 1987; Johnston and Einstein, 1990; Baig and Urbancic, 2013; Maghsoudi et al., 2014; 2016).

The PDF following (10) reads

$$f(M) = \begin{cases} \lambda\beta_1 e^{-\beta_1(M-M_{min})} & \text{for } M \leq M_t \\ \mu\beta_2 e^{-\beta_2(M-M_{min})} & \text{for } M > M_t \end{cases} \quad (11)$$

$$\text{where } \lambda = \left(1 - \left(1 - \frac{\beta_1}{\beta_2}\right) e^{-\beta_1(M_t - M_{min})}\right)^{-1}, \quad \mu = \lambda \frac{\beta_1 e^{-\beta_2(M_t - M_{min})}}{\beta_2 e^{-\beta_1(M_t - M_{min})}}.$$

We used the bi-exponential model with the parameters  $b_1 \in [0.7, 1.3]$ ,  $b_2 = 2 - b_1$ ,  $b = \beta \ln 10$ ,  $M_{min} = 0.5$ ,  $M_t = 2.0$  (Figure 2).

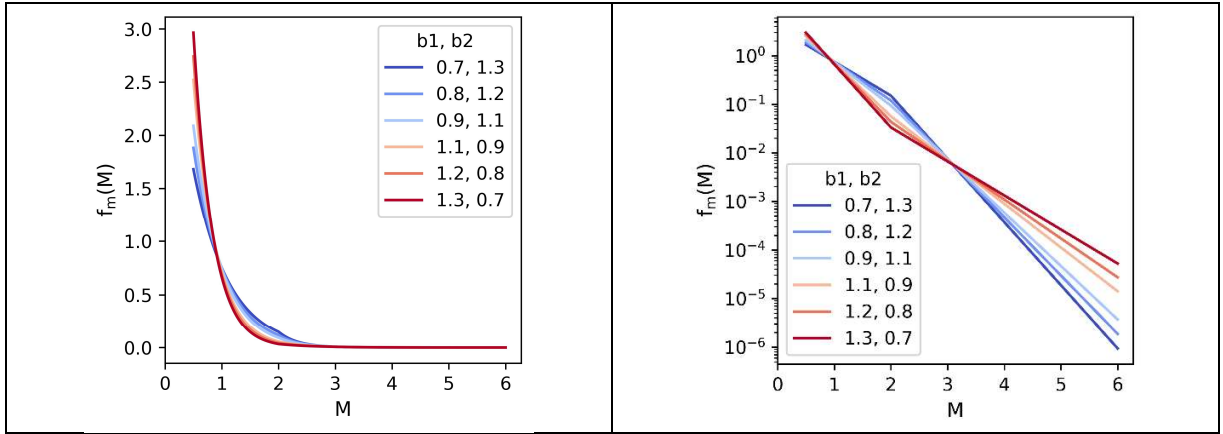


Figure 2 Bi-exponential distribution models used to generate synthetic catalogs.

### Exponential-Gaussian Distribution

For the last type of distribution used to generate synthetic data, we used a combination of exponential and Gaussian distributions. This combined type of distribution can be used to model the effect of characteristic earthquakes hypothesized and observed in tectonic seismicity (e.g., Wesnousky et al., 1983; Schwartz and Coppersmith, 1984; Jackson and Kagan, 2014; Parsons et al., 2018), but also observed in anthropogenic seismicity (e.g. Eaton et al., 2014; Igonin et al., 2018). The model PDF reads

$$f(M) = p\beta e^{-\beta(M-M_{min})} + \frac{1-p}{\sqrt{2\pi}\sigma} e^{-\frac{(M-M_t)^2}{2\sigma^2}} \quad (12)$$

We used this model with the parameters  $b = \beta \ln 10$  for  $b = 1.0$ ,  $M_{min} = 0.5$ ,  $M_t = 3.0$ ,  $\sigma = 0.3$ ,  $p = 0.85, 0.9$ , and  $0.95$  (Figure 3)

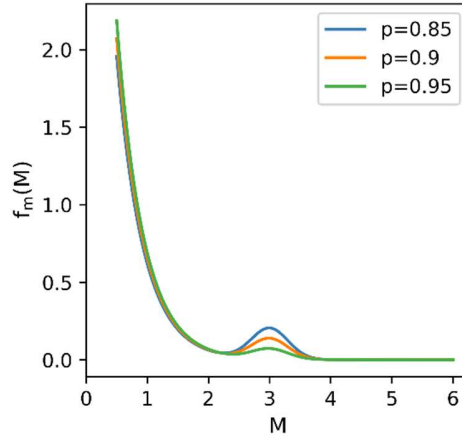


Figure 3 Exponential-Gaussian distribution models used to generate synthetic catalogs.

## Simulation Experiments

We took between 50 and 5000 samples from each probability distribution. This was repeated to obtain  $10^5$  independent simulation experiments for each distribution.

We were looking for solutions primarily for human-induced seismicity, which is weak compared to tectonic earthquakes, though the hazard posed by this anthropogenic seismicity can be considerable. Nevertheless, depending on the inducing technological processes, the well-documented maximum size of anthropogenic seismic events is between magnitudes 4 and 6 (Lasocki and Orlecka-Sikora, 2021). Therefore, we restricted the samples and subsequent analysis to the range beginning at  $M_{min} = 0.5$  and ending at  $M = 6$ .

We applied the five adaptive KDE methods for each simulation to obtain an estimated PDF  $\hat{f}$  for each method for each simulation. Each PDF,  $\hat{f}$ , was then used to obtain the cumulative distribution function (CDF) estimates,  $\hat{F}$ , by integration:

$$\hat{F}(x) = \int_{-\infty}^x \hat{f}(t) dt \quad (13)$$

Then, we calculated the mean integrated squared error (MISE) to determine the discrepancy between the actual distribution and the estimate:

$$\text{MISE}(KDE) = \mathbf{E} \left[ \int \left( \hat{F}(M) - F(M) \right)^2 dM \right], \quad (14)$$

where  $F$  was the true CDF of the distribution from which the samples were drawn and  $\hat{F}$  was the CDF obtained through estimation. The performance of each KDE method was settled by the MISE over all  $10^5$  simulations. Smaller  $\text{MISE}(KDE)$  signified a better KDE estimation method.

We also fit the exponential model (1) to the simulated samples using the maximum likelihood estimation (MLE) method and calculated related  $\text{MISE}(EXP)$  using in (14) the exponential estimate of CDF,  $\hat{F}_{exp}(M)$ , and the CDF of the actual underlying distribution model,  $F$ . The relation  $\text{MISE}(KDE) < \text{MISE}(EXP)$  indicated that the KDE method outperformed the estimation based on the G-R relation-led exponential model and vice versa.

The primary purpose of this study was to find the most suitable KDE method for seismic hazard assessments. The mean return period (MRP) is one of the most widely used parameters of seismic hazard as it is the average time between successive earthquakes with magnitude  $M$  or higher, assuming that the earthquake-generating process is Poissonian:

$$\text{MRP}(M) = \frac{1}{\lambda(1-F(M))} \quad (15)$$

where  $\lambda$  is the activity rate of events with a magnitude greater than or equal to the magnitude of completeness, and  $F(M)$  is the CDF of these events. For our synthetic catalogs, we assumed  $\lambda$  with a value of 20 events per day. We then took the mean of the estimated CDFs and used (15) to calculate the MRP.

## Results and Discussion

We are looking for solutions applicable to seismic hazard analysis that focus on larger magnitude events that can cause damage. For this reason, we pay particular attention to the accuracy of the estimates of both CDF and MRP for larger magnitudes. Therefore, although we generated synthetic catalogs starting from magnitude  $M_{min} = 0.5$ , we present here the results concerning magnitudes at and

above 2 for a sample size of 400 or more. These sample sizes ensure a non-negligible probability of a magnitude  $\geq 2.0$  occurrence in the generated samples. For results across the full magnitude range and all sample sizes, please see Appendix 2.

### Exponential Distribution

The results when the underlying distribution is exponential (1) are shown in Figure 4 – the quality of estimations expressed in terms of MISE (14), and Figure 5 – the MRP (15).

When exact parametric data models are known, MLE outperforms nonparametric estimation methods. Therefore, it is not surprising that when an exponential distribution underlies the data, in Figure 4,  $MISE(EXP) < MISE(KDE)$  for every KDE method. However, the MISE values of the parametric MLE method and all of the KDE methods are small. The largest MISE values occur when the sample size is smallest and  $b=0.7$  – about  $10^{-5}$  for MLE and  $4 \times 10^{-5}$  for Scott's rule (the KDE method with the largest MISE value observed).

Among the KDE methods, diffKDE and ISJ have nearly the same performance. The performance of Silverman's method is similar to those three mentioned when  $b$  is smallest ( $b=0.7$ ), that is, when the range of larger magnitudes is best populated. For other values of  $b$ , the performance of Silverman's method worsens. As the sample size increases, the quality of estimation of all studied methods increases, which is expressed by the decrease in MISE.

As expected, the MRP based on the MLE estimated CDF is practically the same as that calculated from the CDF of the model. The MRP plot in Figure 5 shows the black line from the model completely overlapping the red line from MLE. However, it is worth noting that the MRP based on diffKDE (the gray line) is nearly identical to the previous two. A slight discrepancy appears only for the simulated data with  $b=1.3$  in the largest magnitude range between 5 and 6. This result suggests that when a sample is suitably

big (here, 1000), diffKDE can be safely used in hazard analysis even if the magnitude data follows the Gutenberg-Richter relation and the exponential distribution model.

In Figure 4, the MISE of diffKDE and ISJ are nearly indistinguishable. In Figure 5, the MRPs of the two are distinctly visible from each other. The distribution of MISE is asymmetric in each case. Estimation methods may differ strongly in their MISE distributions but only slightly in their MISE values. Therefore, the MISE comparison allows conclusions to be drawn about the performance of the studied estimation methods but may not correctly report the consequences for hazard estimates. The MISE and the mean MRP should both be taken into consideration.

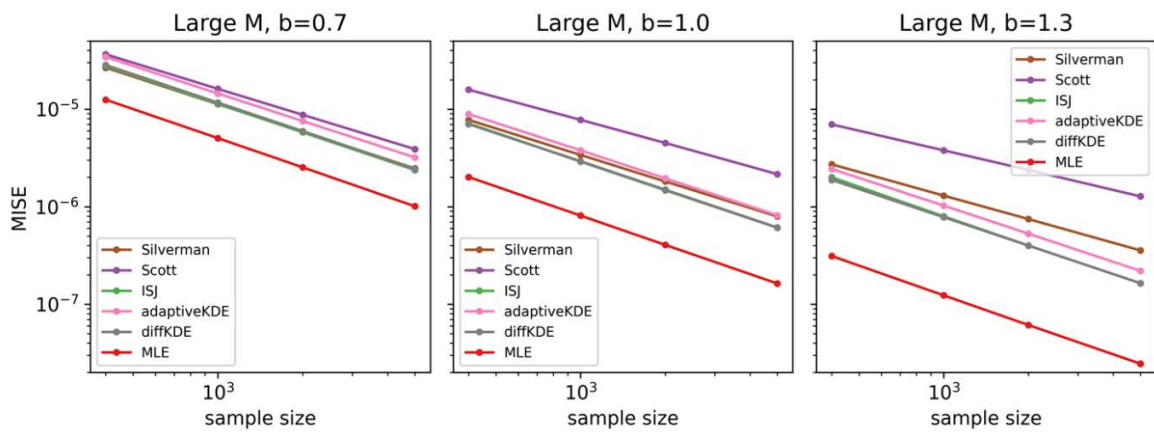


Figure 4 MISE results for the data drawn from the exponential distribution (1) with  $b=0.7$  – left,  $b=1.0$  – middle, and  $b=1.3$  – right. Colors mark the KDE methods of CDF estimation and the MLE estimate of CDF assuming the exponential distribution model (red).

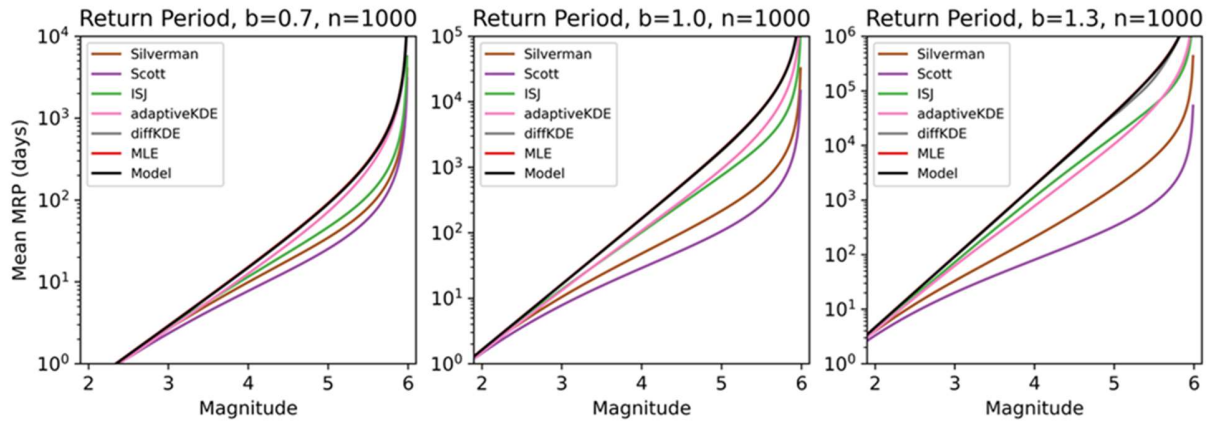


Figure 5 MRP for the 1000 magnitude values drawn from the exponential distribution (1) with  $b = 0.7$  – left,  $b=1.0$  – middle, and  $b=1.3$  – right. Colors mark MRPs for CDFs obtained from the studied KDE methods, for CDF from the MLE assuming the exponential distribution model (MLE - red), and for the CDF of data distribution (Model - black).

### Bi-exponential Distribution

In the following experiment, data was drawn from non-exponential distributions with increasing deviations from exponentiality. These deviations are not dramatic and can be found in actual observations of anthropogenic seismicity (Kostoglou et al., 2024). In addition to the study of the performance of KDE methods, we also investigated what happens when the estimation is based on the assumption of an exponential model, which is incorrect in this case.

The MISE (14) results when the data distribution is bi-exponential (10-11) are shown in Figure 6 – concave bi-exponential and Figure 7 – convex bi-exponential. The MRPs (15) for the studied bi-exponential distributions are shown in Figures 8 – concave and 9 – convex.

In every instance, diffKDE outperforms the other KDE methods. Its performance practically does not change when the data distribution deviates more from exponentiality ( $\text{abs}(b_1 - b_2)$  increases). The ISJ method performs almost as well as diffKDE. As sample size increases, the MISEs of the KDE methods decrease.

The distribution from which the data was drawn is not exponential and so an exponential parametric model is incorrect. For this reason, the MISE values of the MLE method are greater than the MISE values of the diffKDE method (except when the sample size is 400 or smaller). With an increasing sample size, the difference in these MISE values becomes very big because the sample size has minimal effect on the performance of MLE. Its MISE values are mostly related to the deviation of the actual distribution data from the exponential model. For samples of 400 elements drawn from the concave distribution closest to an exponential distribution ( $\text{abs}(b_1 - b_2) = 0.4$ ), the performance of MLE and diffKDE were similar. For the convex distribution closest to an exponential distribution ( $\text{abs}(b_1 - b_2) = 0.1$ ), MLE outperforms diffKDE method a bit at sample size 400.

The diffKDE method also provided the most accurate estimates of mean MRP out of all the KDE methods (Figures 8 and 9). In fact, these diffKDE estimates are difficult to distinguish visually from the actual (model) MRPs, meaning diffKDE is correctly estimating the seismic hazard.

Using MLE based on an incorrect (exponential) model while the data distribution is bi-exponential leads to very significant discrepancies between the actual and estimated MRPs (Figures 8 and 9). This effect is particularly dramatic for data drawn from the concave bi-exponential distributions. For the case of ( $b_1 = 1.3, b_2 = 0.7$ ), the true MRP for a magnitude 4 event is around 60 days compared to the MLE estimate of around 1000 days. The hazard is significantly underestimated.

For the convex case, the differences between the true MRPs and those obtained from MLE are smaller but still very significant, and the hazard is overestimated. Even for the distribution closest to an exponential ( $b_1 = 0.9, b_2 = 1.1$ ), the estimated MRP of a magnitude 4 event is more than double the true MRP (90 versus 200 days).

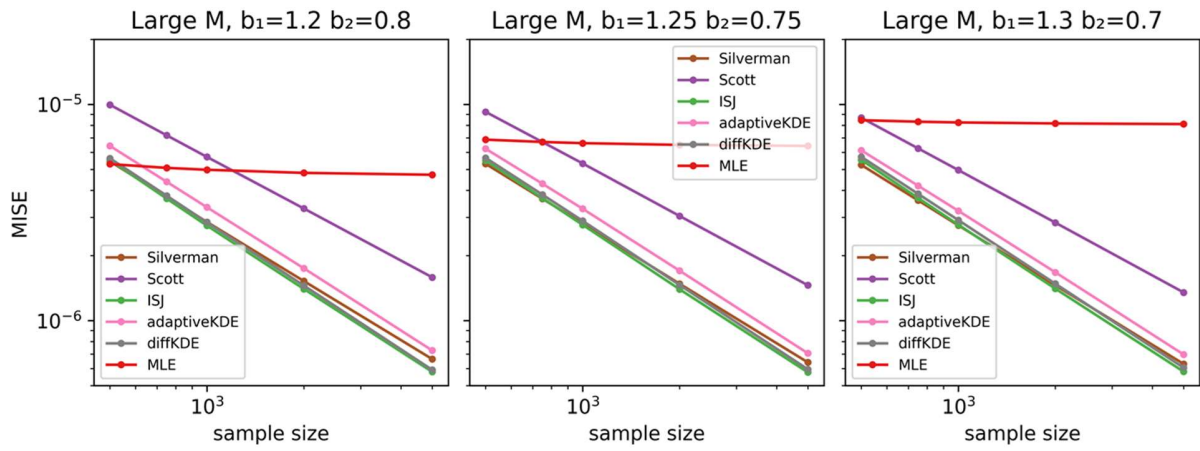


Figure 6 MISE results for the data drawn from the concave bi-exponential distribution (10 - 11) with  $b_1 = 1.2$  – left,  $b_1 = 1.25$  – middle, and  $b_1 = 1.3$  – right, where  $b_2 = 1 - b_1$ . Colors mark the KDE methods of CDF estimation and the MLE estimate of CDF assuming the exponential distribution model (red).

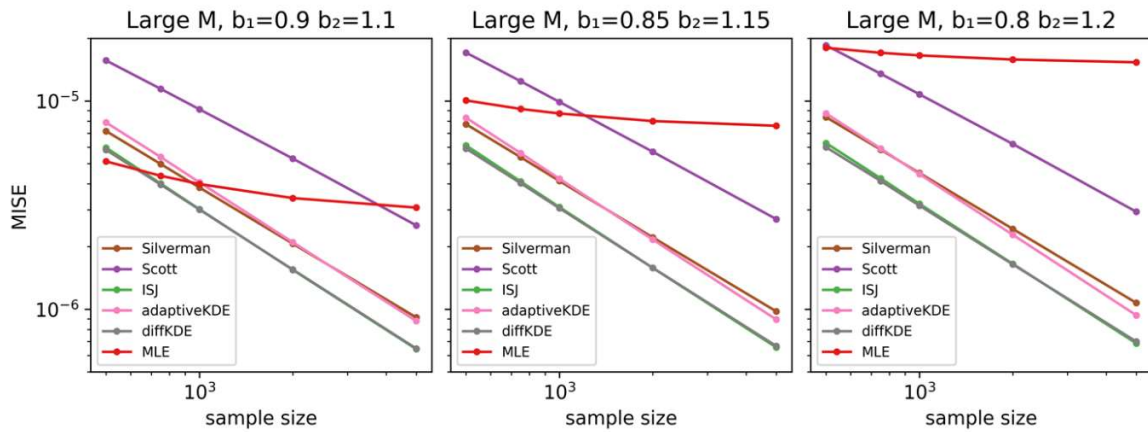


Figure 7 MISE results for the data drawn from the convex bi-exponential distributions (10 - 11) with  $b_1 = 0.9$  – left,  $b_1 = 0.85$  – middle, and  $b_1 = 0.8$  – right, where  $b_2 = 1 - b_1$ . Colors mark the KDE methods of CDF estimation and the MLE estimate of CDF assuming the exponential distribution model (red).

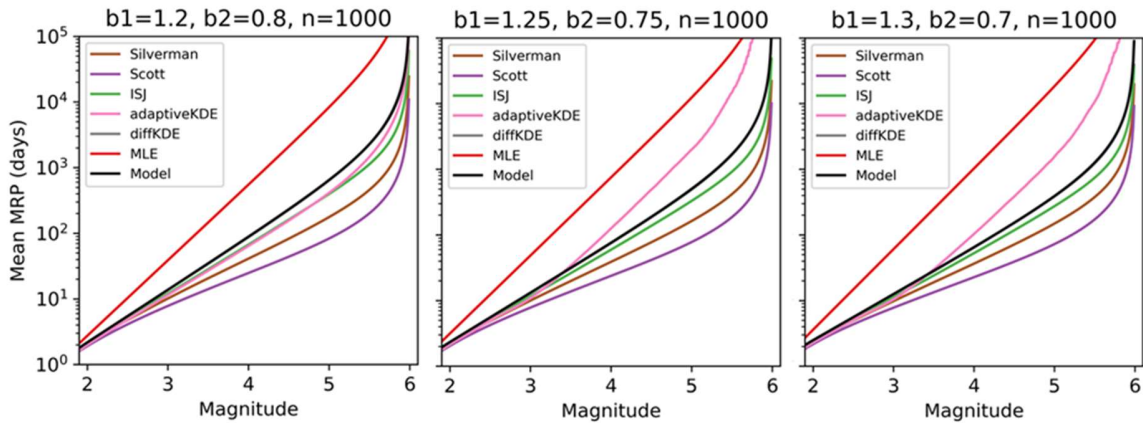


Figure 8 Mean MRP using 1000 magnitude values drawn from the concave bi-exponential distribution (10-11) with  $b_1 = 1.2$  – left,  $b_1 = 1.25$  – middle, and  $b_1 = 1.3$  – right, where  $b_2 = 1 - b_1$ . Colors mark MRPs for CDFs obtained from the studied KDE methods, for CDF from the MLE assuming the exponential distribution model (MLE - red), and for the CDF of the data distribution (Model - black).

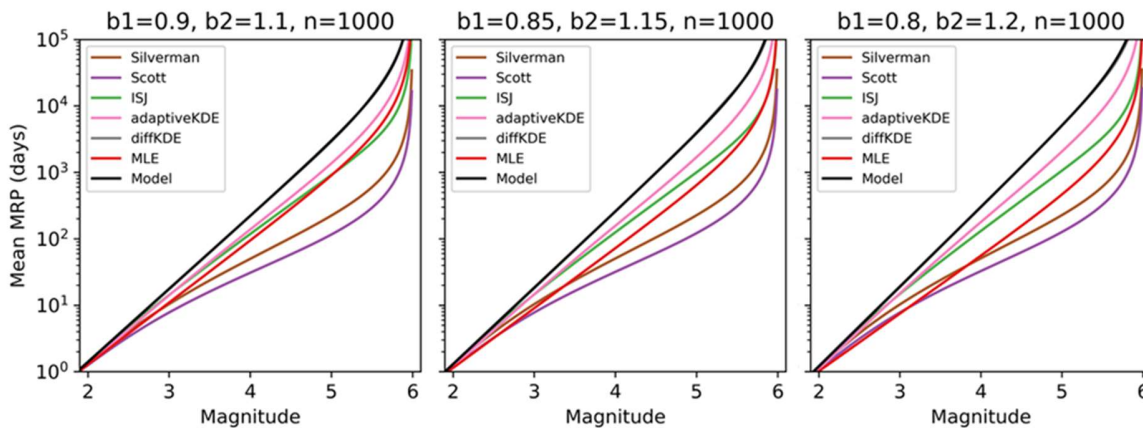


Figure 9 Means MRP using 1000 magnitude values drawn from the convex bi-exponential distributions (10-11) with  $b_1 = 0.9$  – left,  $b_1 = 0.85$  – middle, and  $b_1 = 0.8$  – right, where  $b_2 = 1 - b_1$ . Colors mark MRPs for CDFs obtained from the studied KDE methods, for CDF from the MLE assuming the exponential distribution model (MLE - red), and for the CDF of data distribution (Model - black).

### Exponential-Gaussian Distribution

The results obtained using the exponential-Gaussian distribution are shown in Figures 10 (MISE) and 11 (MRP). Here, the performance of all KDE methods (except Scott's) are comparable. DiffKDE achieves the smallest MISE, except when the sample size is greater than 3000. In this case, adaptiveKDE performs the best, yet the differences in MISE are minor. As the Gaussian content increases to 10% ( $\rho=0.9$ )

then 15% ( $p=0.85$ ), the relative improvement of using adaptiveKDE over the other methods increases. However, MISE values still increase with increasing Gaussian content in the model, regardless of the estimation method used.

In the 1000-element sample case shown in Figure 11, the MRP estimated from diffKDE nearly overlaps the actual MRP (model). The most significant discrepancies between the two occur when the Gaussian content of the distribution reaches 15% ( $p=0.85$ ).

Compared to the KDE results, the estimates using MLE based on an exponential distribution model are significantly worse (Figure 10). The large MISE values are due to the incorrectness of the distribution model; they do not depend on sample size but do increase with the increasing Gaussian part of the mixed data distribution. As a result, the MRP calculated based on MLE estimates of the CDF differs dramatically from the actual MRP (Figure 11). The hazard is overestimated. For a magnitude 4 event, in the worst case of  $p=0.85$ , the MLE estimate of the MRP is 8 days but the actual MRP is around 200 days.

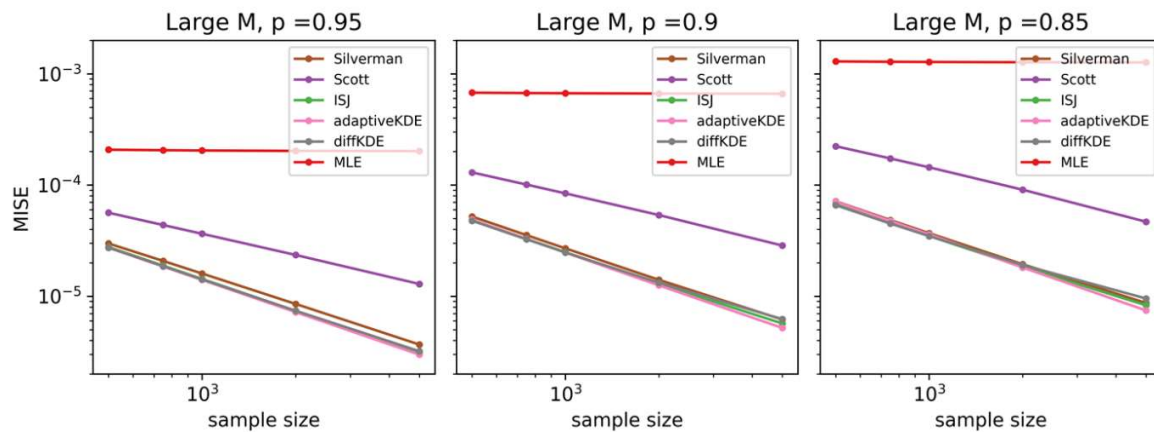


Figure 10 MISE results for the data drawn from the exponential-Gaussian distribution (12) with  $p = 0.95$  – left,  $p = 0.9$  – middle, and  $p = 0.85$  – right. Colors mark the KDE methods of CDF estimation and the MLE estimate of CDF assuming the exponential distribution model (red).

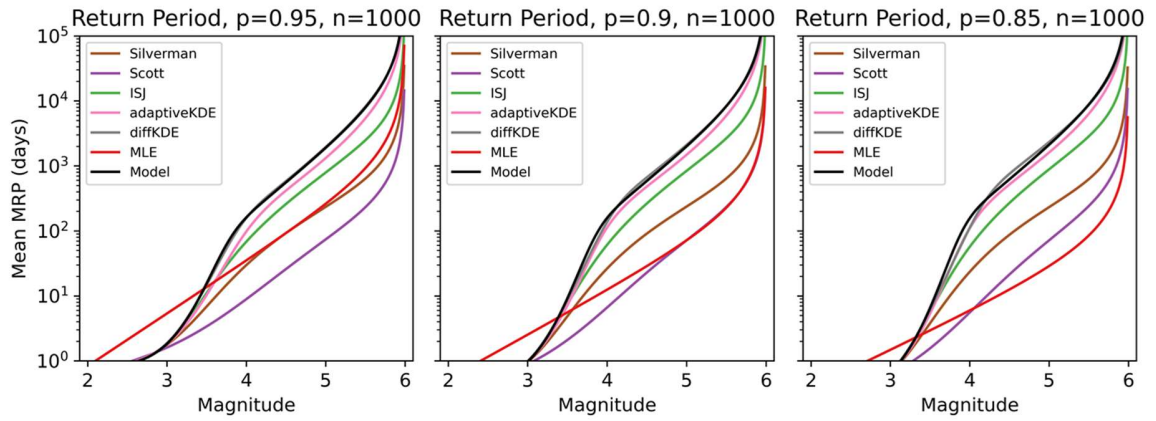


Figure 11 Mean MRP for the 1000 magnitude values drawn from the exponential-Gaussian distribution (12) with  $p = 0.95$  – left,  $p = 0.9$  – middle, and  $p = 0.85$  – right. Colors mark MRPs for CDFs obtained from the studied KDE methods, for CDF from the MLE assuming the exponential distribution model (MLE - red), and for the CDF of the data distribution (Model - black).

## Conclusions

Of the five KDE methods tested, diffKDE provides the most accurate estimate of the cumulative distribution function of magnitude in the range of large magnitudes. Since large magnitude events are of primary concern in seismic hazard analysis, we conclude that diffKDE is the most suited for probabilistic seismic hazard assessment out of these five methods.

When the distribution that underlies data is known, parametric distribution estimation methods, especially the maximum likelihood estimation method, outperform nonparametric ones including KDE methods. However, our studies showed that for samples drawn from an exponential distribution of 1000 elements or more – a condition not unusual in anthropogenic seismicity - the diffKDE method provides a seismic hazard estimate, expressed by the mean return period, of accuracy practically the same as the accuracy of a MLE estimate based on the exponential distribution model. However, when the distribution that underlies the data deviates from exponentiality, using the exponential model of magnitude distribution results in very inaccurate hazard estimates, whose practical consequences can be severe. In contrast, hazard estimates using the diffKDE method agree well with actual hazard values. Therefore, considering that the magnitude distribution of anthropogenic seismicity often deviates from the exponential distribution, we recommend that the diffKDE estimation method be used in probabilistic seismic hazard assessment whenever there is anthropogenic seismicity with a reasonable sample size of events.

## Appendix 1 - Computational Implementation

The KDE methods mentioned above were implemented as Python packages by various authors. We applied their codes to our data sets.

- 1) Silverman, Scott, ISJ with and without Abramson's adaptive bandwidth

Available as a Python package at: <https://pypi.org/project/arviz/>

Reference paper:

Kumar et al., (2019). ArviZ a unified library for exploratory analysis of Bayesian models in Python. Journal of Open Source Software, 4(33), 1143, <https://doi.org/10.21105/joss.01143>

- 2) adaptiveKDE

Available as a Python package at: <https://pypi.org/project/adaptivekde/>

Reference paper:

H. Shimazaki and S. Shinomoto, "Kernel Bandwidth Optimization in Spike Rate Estimation," in Journal of Computational Neuroscience 29(1-2): 171–182, 2010 <http://dx.doi.org/10.1007/s10827-009-0180-4>.

- 3) DiffKDE

Available as a Python package at: <https://doi.org/10.5281/ZENODO.7594915>

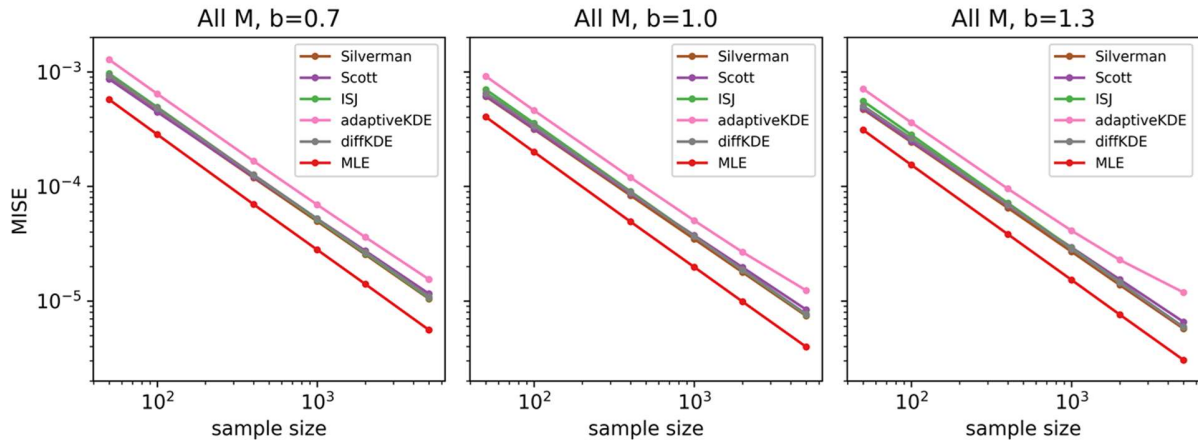
Reference paper:

Pelz, M.-T., Schartau, M., Somes, C. J., Lampe, V., and Slawig, T.: A diffusion-based kernel density estimator (diffKDE, version 1) with optimal bandwidth approximation for the analysis of data in geoscience and ecological research, Geosci. Model Dev., 16, 6609–6634, 2023 <https://doi.org/10.5194/gmd-16-6609-2023>

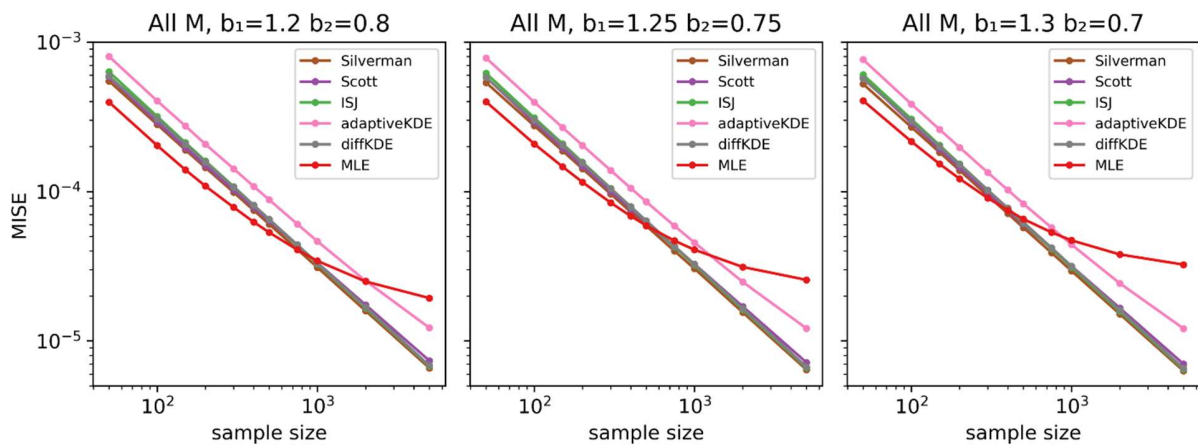
## Appendix 2 – MISE across at all magnitudes

Figures of MISE for the full magnitude range of 0.5 to 6

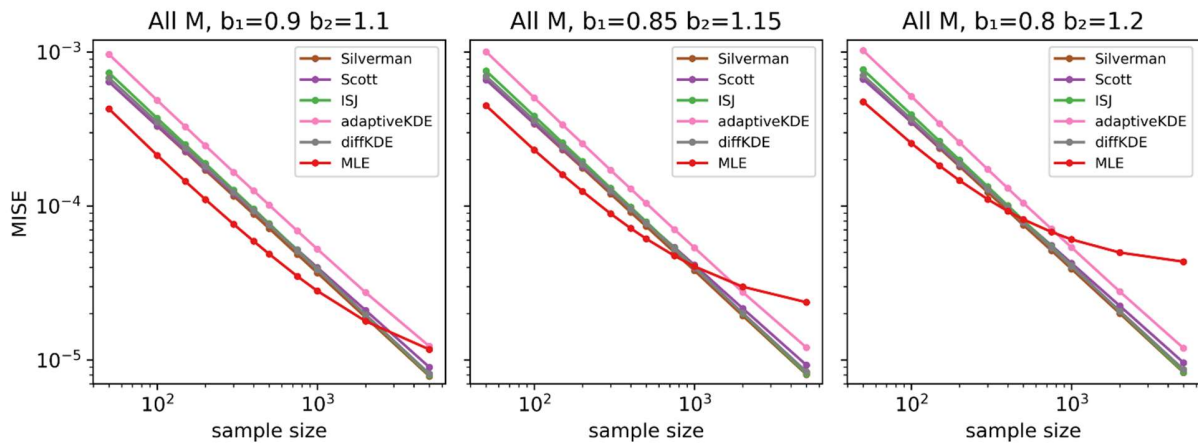
### Exponential Distribution



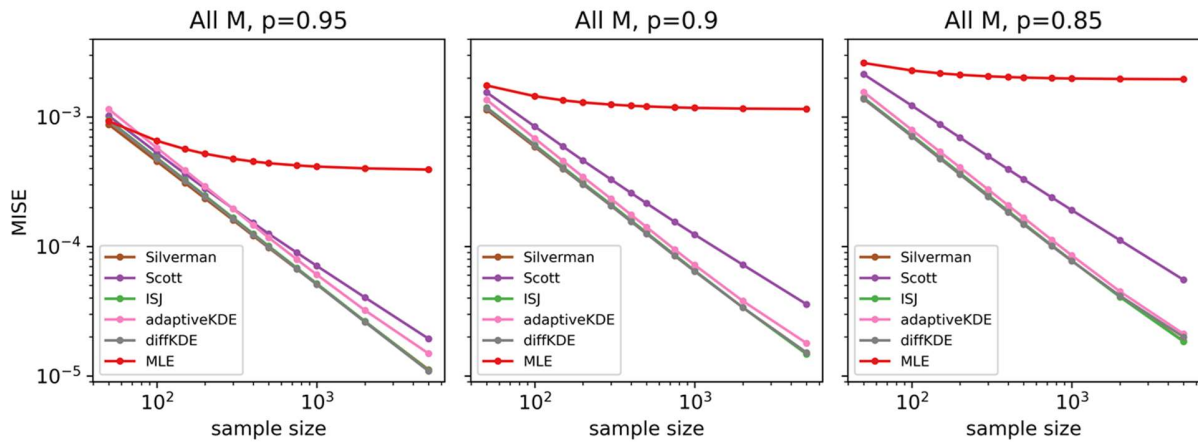
### Bi-Exponential Distribution – concave case



## Bi-Exponential Distribution – convex case



## Exponential Gaussian Distribution



## Acknowledgements

We acknowledge the CINECA award under the ISCRA initiative, for the availability of high performance computing resources and support. The work presented in this paper was supported by the project DT-Geo funded by Horizon Europe under the grant agreement No 101058129.

## References

- Abramson, I.S. 1982. On bandwidth variation in kernel estimates – a square root law. *The Annals of Statistics* 10(4), 1217-1223
- Baig, A.M., and T. Urbancic (2013) Utilizing fracture complexity and stress release parameters to characterize b-value behavior and the growth of hydraulic fractures. SEG Technical Program Expanded Abstracts 2013, DOI: 10.1190/segam2013-1420.1
- Botev, Z. I., J. F. Grotowski, and D. P. Keroese (2010) Kernel density estimation via diffusion. *The Annals of Statistics* 38(5), 2916-2957, doi: 10.1214/10-AOS799
- Breiman, L., W. Meisel, and E. Purcell (1977). Variable Kernel Estimates of Multivariate Densities. *Technometrics*, 19(2), 135–144. <https://doi.org/10.2307/1268623>
- Eaton, D.W., J. Davidsen, P.K. Pedersen, and N. Boroumand (2014) Breakdown of the Gutenberg-Richter relation for microearthquakes induced by hydraulic fracturing: influence of stratabound fractures. *Geophysical Prospecting* 62, 806–818, doi: 10.1111/1365-2478.12128
- Gutenberg, B., and C. F. Richter, *Seismicity of the Earth and Associated Phenomena*, (Princeton University Press, Princeton, 1954)
- Igonin, N., M. Zecevic, and D.W. Eaton (2018). Bilinear magnitude-frequency distributions and characteristic earthquakes during hydraulic fracturing. *Geophysical Research Letters*, 45, 12,866–12,874. <https://doi.org/10.1029/2018GL079746>
- Izenman, A.J. (1991) Review Papers: Recent Developments in Nonparametric Density Estimation, *Journal of the American Statistical Association*, 86:413, 205-224, DOI: 10.1080/01621459.1991.10475021
- Jackson, D.D., and Y.Y. Kagan (2011). Characteristic earthquakes and seismic gaps. In: Gupta, H.K. (eds) *Encyclopedia of Solid Earth Geophysics*. *Encyclopedia of Earth Sciences Series*. Springer, Dordrecht. [https://doi.org/10.1007/978-90-481-8702-7\\_181](https://doi.org/10.1007/978-90-481-8702-7_181)
- Johnston, J.C., and H.H. Einstein (1990) A survey of mining associated rockbursts, In *Rockbursts and Seismicity in Mines* (ed. Fairhurst, C.) (Balkema, Rotterdam), pp. 121-128.
- Kijko, A., B. Drzęźła, and T. STANKIEWICZ (1987), Bimodal character of the distribution of extreme seismic events in Polish mines, *Acta Geophys. Pol.* 35, 157-166.
- Kijko, A., S. Lasocki, and G. Graham, Non-parametric Seismic Hazard in Mines. *Pure Appl Geophys* 158, 1655–1675, 2001
- Kostoglou, A., B. Orlecka-Sikora, S. Lasocki, and F. Tong, The Gutenberg-Richter relation may not hold for the anthropogenic seismicity. 2024
- Lasocki, S., and B. Orlecka-Sikora, B. Seismic hazard assessment under complex source size distribution of mining-induced seismicity. *Tectonophysics* 456, 28–37, 2008.
- Lasocki, S.; Orlecka-Sikora, B. Anthropogenic Seismicity Related to Exploitation of Georesources. In *Encyclopedia of Solid Earth Geophysics*; Gupta, H., Ed.; *Encyclopedia of Earth Sciences Series*; Springer: Cham, Switzerland, 2020.

- Loftsgaarden, D.O., and C.P. Quesenberry (1965) A Nonparametric Estimate of a Multivariate Density Function. *Ann. Math. Statist.* 36(3), 1049-1051 DOI: 10.1214/aoms/1177700079
- Maghsoudi, S., S. Hainzl, S. Cesca, T. Dahm, and D. Kaiser (2014) Identification and characterization of growing large-scale en-echelon fractures in a salt mine. *Geophys. J. Int.* 196, 1092–1105, doi: 10.1093/gji/ggt443
- Maghsoudi, S., D. W. Eaton, and J. Davidsen (2016), Nontrivial clustering of microseismicity induced by hydraulic fracturing, *Geophys. Res. Lett.*, 43, 10,672–10,679, doi:10.1002/2016GL070983
- Okal, E.A., and B.A. Romanowicz (1994) On the variation of *b*-values with earthquake size. *Physics of the Earth and Planetary Interiors* 87, 55–76.
- Pacheco, J.F., C.H. Scholz, and L.R. Sykes (1992) Changes in frequency–size relationship from small to large earthquakes. *Nature* 355.6355: 71-73.
- Parsons, T., E.L. Geist, R. Console, and R. Carluccio (2018). Characteristic earthquake magnitude frequency distributions on faults calculated from consensus data in California. *Journal of Geophysical Research: Solid Earth*, 123, 10,761–10,784. <https://doi.org/10.1029/2018JB016539>
- Pelz, M.-T., Schartau, M., Somes, C. J., Lampe, V., and Slawig, T.: A diffusion-based kernel density estimator (diffKDE, version 1) with optimal bandwidth approximation for the analysis of data in geoscience and ecological research, *Geosci. Model Dev.*, 16, 6609–6634, 2023 <https://doi.org/10.5194/gmd-16-6609-2023>
- Schwartz, D. P., and K.J. Coppersmith (1984). Fault behavior and characteristic earthquakes: Examples from the Wasatch and San Andreas Fault zones. *Journal of Geophysical Research*, 89(B7), 5681–5698. <https://doi.org/10.1029/JB089iB07p05681>
- Scott, D.W. (1992) *Multivariate Density Estimation. Theory, Practice and Visualization*. New York: Wiley.
- Shimazaki, H. and S. Shinomoto (2010) Kernel Bandwidth Optimization in Spike Rate Estimation, *J Comput Neurosci* 29, 171–182, <http://dx.doi.org/10.1007/s10827-009-0180-4>.
- Silverman, B. W., *Density Estimation for Statistics and Data Analysis*, (Chapman Hall, London 1986)
- Sornette, A., and D. Sornette (1999) Renormalization of earthquake aftershocks. *Geophys Res Lett.* 26(13), 1981-1984.
- Terrell, G.R and D.W. Scott, 1992. Variable Kernel Density Estimation, *The Annals of Statistics* 20(3), 1236-1265.
- Utsu, T. (1999) Representation and analysis of the earthquake size distribution: a historical review and some new approaches. *Pure Appl. Geophys.* 155, 509–535
- Wesnousky, S. G., C. H. Scholz, K. Shimazaki, and T. Matsuda (1983) Earthquake frequency distribution and the mechanics of faulting, *J. Geophys. Res.*, 88, 9331– 9340